Colloid Polym Sci 278:425–433 (2000)

ORIGINAL CONTRIBUTION

H. Motschmann
R. Teppner
S. Bae
K. Haage
D. Wantke

What do linear and nonlinear optical techniques have to offer for the investigation of adsorption layers of soluble surfactants?

Received: 13 September 1999
Accepted: 24 November 1999

Presented at the 39th General Meeting of the Kolloid-Gesellschaft, Würzburg, 27–30 September 1999

H. Motschmann (✉) · R. Teppner
S. Bae · K. Haage · D. Wantke
Max Planck Institute of Colloids and Interfaces, D-14424 Potsdam, Germany

e-mail:
hubert.motschmann@mpikg-golm.mpg.de

Abstract In this contribution the potential and the limitation of ellipsometry and surface second-harmonic generation (SHG) for the characterization of adsorption layers of soluble surfactants are discussed with the aid of exemplary measurements carried out with a SHG-active amphiphile. SHG provides an intrinsic surface specifity and the analysis of polarization-dependent SHG measurements yields the symmetry of the interface and the number density and the orientation of the amphiphile. These data can be used to assess some peculiar features of adsorption layers of soluble surfactants. The experimental work focuses on two items: the linear range observed in the $\sigma(c)$ isotherm and the correct description of ionic amphiphiles. In the case of our model system major deviations were found between optical data and data obtained using the Gibbs model. The observed discrepancies could be bridged by the introduction of a coupling between cation and anion within the surface layer in the derivation of the Gibbs equation. The model system was also used to assess the meaning of ellipsometric measurements for the characterization of adsorption layers of soluble surfactants.
In the ultra-thin-film limit an ellipsometric experiment yields only a single parameter η. Usually η is proportional to the amount adsorbed; however, for adsorption layers of soluble surfactants (layer thickness $h < 2$ nm, dielectric constant $\epsilon \approx 2$) none of the underlying assumptions required to establish the direct proportionality from first principles (Maxwell's equations) are met. It is not obvious what η represents under these conditions. The comparison between ellipsometric and SHG data showed that η is not necessarily proportional to the amount adsorbed. The ellipsometric isotherm even possesses a maximum at an intermediate bulk concentration far below the critical micelle concentration. Hence, we have to conclude that ellipsometry is not a suitable alternative to surface tension measurements, neutron reflectometry or nonlinear optical investigations for the determination of the surface excess of soluble surfactants although it is a convenient and valuable tool to monitor qualitatively local and temporal variations of the molecular density at fluid interfaces.

Key words Ellipsometry · Second harmonic generation · Soluble surfactants · Gibbs equation · Surface excess · Adsorption

Introduction

Adsorption layers of soluble amphiphiles determine the properties of a great variety of objects studied in the field of colloidal science and are responsible for such diverse phenomena as foams or micelles [1]. Depending on the choice of the amphiphile emulsions can be stabilized or destabilized. In many industrial applications it is crucial to deliberately control and modify the interfacial properties of fluids. Obviously, this task requires an understanding of the prevailing interactions and the static and dynamic properties of adsorption layers at liquid–liquid or liquid–air interfaces. Good reviews can be found in Refs. [2, 3].

The experimentalist faces some inherent difficulties. The properties of the air–water or the oil–water interface limit the number of analytical techniques which can be applied and many powerful methods such as X-ray diffraction or reflection or all techniques based on scattering of charged particles, such as high-resolution electron energy loss spectroscopy, cannot be used for obvious reasons. Furthermore, the number density of the amphiphile within the adsorption layer is fairly low. Even if a sufficiently high sensitivity is achieved the conclusion may be of limited value since the interfacial region and the bulk region contain the very same species which both contribute to the signal. Hence, besides submonolayer sensitivity the ideal surface analytical tool should provide intrinsic discrimination between bulk and interfacial regions.

Due to these peculiarities many studies have focused on surface tension measurements. The equilibrium surface tension is measured as a function of the concentration of the amphiphile. The isotherm is then discussed using a suitable thermodynamic model which yields the area per molecule and the surface excess along with some thermodynamic quantities, for instance, the free enthalpy of adsorption or the lateral interaction parameter. At this point a comparison with insoluble monolayers might be worthwhile [4]. Langmuir monolayers are quasi-two-dimensional systems and the mean area per molecule is simply given by two experimental parameters: the total accessible surface area and the amount of amphiphile spread at the surface; however, adsorption layers of soluble amphiphiles are formed by spontaneous adsorption and the prevailing exchange of amphiphiles between bulk and interfacial areas makes a comparable calculation impossible. All quantities can only be obtained by a suitable thermodynamical model and there is some controversy about the correct equation of state and the validity of the underlying assumptions (Frumkin two-state model) [5, 6].

All these equations of state are based on some modifications of the Gibbs equation. The Gibbs equation can be derived by first principles [1, 7]. It relates the surface excess, Γ, to the equilibrium surface tension, σ_e, of the dilute aqueous surfactant solution. In the derivation the interfacial region is treated as a separate phase and the equilibrium conditions for the chemical potentials of all components in all phases lead to

$$\Gamma = -1/(mRT)\left(\frac{\partial\sigma_e}{\partial\mu}\right)_T = -1/(mRT)\frac{d\sigma_e}{d\ln a} \approx -1/(mRT)\frac{d\sigma_e}{d\ln c} \quad , \tag{1}$$

where μ is the chemical potential of the solute component in the bulk solution, m is the number of independent components, a is the activity of the solute and c is the corresponding concentration. Usually it is justified to replace the activity by the bulk concentration since the concentration range is fairly low [1]. In the absence of an indifferent electrolyte the rigorous thermodynamical treatment requires a factor of $m = 2$ for a 1:1 ionic surfactant. A factor of $m = 2$ appears to be taken for granted in the literature; however, the corresponding molecular picture makes this questionable. A value of $m = 2$ implies the same contribution of anion and cation to the surface tension, σ. In general, both differ in size and surface activity. A clarification of this issue requires the measurement of the surface excess by techniques independent of thermodynamic considerations.

The adsorption isotherms of many soluble surfactants possess some peculiar features. Many groups report a linear relation between surface excess and log c. This was confirmed for a great variety of chemically different amphiphiles and seems to be an intrinsic feature of these systems [8–10]. The reported linear dependence means that the surface excess remains constant, while there is a significant decrease in the surface tension. This finding lead to a vivid discussion and some groups suggested the contribution of the subsurface layer to the surface tension [11]. The experimental determination of quantities such as the elasticity requires even higher derivatives of the isotherm, which leads to a high error in the values obtained.

Hence, the progress in this area of science requires methods which directly probe the interfacial architecture. Optical techniques possess appealing features and good reviews can be found in Refs. [12, 13]. The data accumulation is fast and can be employed at any arbitrary reflecting interface and even the buried oil–water interface can be probed. The aim of this contribution is to discuss the potential and limitation of linear and nonlinear optical techniques, namely ellipsometry and second-harmonic generation (SHG), for the investigation of adsorption layers of soluble surfactants at the fluid–fluid and fluid–air interface.

Theory

Linear optics

The most powerful linear optical technique for the characterization of ultrathin films at fluid interfaces is ellipsometry [14]. It uses the fact that, in general, the state of polarization is changed upon reflection on a film-covered surface. An ellipsometric measurement yields two quantities, Δ and Ψ, which are sensitive to the interfacial architecture. The basic equation of ellipsometry relates both quantities to the complex reflectivity coefficients, r_p and r_s, for $\hat{p}$ and $\hat{s}$ polarized light:

$$\tan \Psi e^{i\Delta} = \frac{r_p}{r_s} \quad . \tag{2}$$

The calculation of reflectivity coefficients of stratified media is straightforward and well documented in the literature. There are sophisticated algorithms which can be easily translated in a computer program. A sound description covering also anisotropic media can be found in the book of Lekner [15]. The inverse problem, namely the evaluation of the film parameters such as the refractive index, n, or the film thickness, h, on the basis of the measured quantities is not trivial and sometimes there is not a unique solution: several (n, h) combinations are in agreement with the experimental data. In favorable cases it is possible to determine n and h to within 1 Å, which is fascinating since the wavelength of the probe is of the order of 5000 Å.

An ellipsometric measurement of monolayers ($h < 2$ nm) yields only a single quantity. The presence of such a monolayer does not change the reflectivity $|r_i|^2$ and hence there are no detectable changes in Ψ. Thus, in this case the data analysis relies only on Δ and unfortunately there is no way to increase the number of independent quantities. Neither a scan of the angle of incidence, α, nor spectroscopic ellipsometry provides independent data sets. A sound treatment of this problem especially dedicated to monolayers at fluid interfaces is given in Ref. [16].

In the thin-film limit (layer thickness $h \ll$ wavelength λ) it is possible to expand the reflectivity coefficients in a power series in terms of h/λ. The first term of the expansion provides a complete description of the optical relectivity properties of monolayers and is known as Drude's equation [15]. Drude's equation relates η to the dielectric constant, ϵ, and h. For isotropic media Drude's equation reads

$$\eta = \int \frac{(\epsilon - \epsilon_1)(\epsilon - \epsilon_2)}{\epsilon} \, \mathrm{d}z \quad . \tag{3}$$

A further simplification of Eq. (3) reveals the physical meaning of η, which is directly proportional to the ellipsometric response, Δ. Quite often, for instance in the case of adsorption of organic compounds onto solid supports, ϵ_2 exceeds ϵ of the monolayer, while $\epsilon \approx \epsilon_1$. Under these conditions Drude's equation can be simplified further:

$$\eta = \frac{\epsilon_1 - \epsilon_2}{\epsilon_1} \int (\epsilon - \epsilon_1) \, \mathrm{d}z \quad . \tag{4}$$

Since a linear relationship between ϵ and the prevailing concentration, c, of segments is well established [17],

$$\epsilon = \epsilon_1 + c \frac{\mathrm{d}\epsilon}{\mathrm{d}c} \quad , \tag{5}$$

a direct proportionality between the experimentally accessible quantity η and the amount adsorbed, Γ, can be derived:

$$\eta = \frac{\epsilon_1 - \epsilon_2}{\epsilon_1} \frac{\mathrm{d}\epsilon}{\mathrm{d}c} \int c \, \mathrm{d}z = \frac{\epsilon_1 - \epsilon_2}{\epsilon_1} \frac{\mathrm{d}\epsilon}{\mathrm{d}c} \Gamma \quad . \tag{6}$$

However, none of these assumptions leading to Eq. (6) hold for the investigation of adsorption layers at fluid interfaces. Drude's equation cannot be simplified and the relation between monolayer data and recorded changes remains obscure. No further simplifications can be achieved on the basis of Fresnel's equations. The ellipsometric measurements may or may not yield the surface excess [18] . In the following we provide experimental evidence that major deviations can occur.

Nonlinear optics

Nonlinear optical techniques combine many of the desired features for the ideal surface analytical tool for the investigation of thin films and in the following we focus on and discuss the potential of surface SHG. SHG is a nonlinear optical $\chi^{(2)}$ process: the generation of frequency-doubled light is the result of the interaction of an intense laser pulse with matter. It has been used for decades to extend the frequency range of laser light sources using noncentrosymmetric crystals. SHG, as a surface-specific tool, exploits the fact that there is no generation of SHG light in centrosymmetric media (strictly speaking this is only valid within the dipole approximation). At the interface of two isotropic media the centrosymmetry is broken and SHG light is generated within the transition region of both adjacent media. Since optical techniques can be applied to any reflecting interface, SHG is a suitable tool for investigating interfacial order in liquid–air, liquid–liquid or liquid–solid interfaces [19, 20].

In favorable cases, the analysis of polarization-dependent SHG measurements allows the determination of the symmetry of the interface, the number density, N, of the amphiphiles and the orientation of the molecules in the interfacial layer. Depending on the hyperpolarizability, β, of the molecules within the adsorption layer,

a submonolayer sensitivity to within $1/50-1/200$ of a monolayer can be achieved, allowing adsorption layers at low surface coverage to be studied. Since SHG provides intrinsic discrimination between the adsorbed monolayer and the bulk phase, it can be used to assess the quantities derived using thermodynamic models [21, 24].

The disadvantage of this technique is that only certain molecules give rise to a SHG signal and in order to fully exploit the potential offered by SHG it is necessary to design a suitable model system with a high hyperpolarizability. The SHG signal is then determined by the dipolar contribution and combinations of various components of the macroscopic susceptibility tensor, $\chi^{(2)}$, are measured in reflection mode. The relation between the individual elements of $\chi^{(2)}$ and the corresponding molecular quantities is provided by the oriented-gas model [25]:

$$\chi^{(2)} \propto \sum_{\text{mol}} \beta \propto N\langle\beta\rangle \ . \tag{7}$$

It states that $\chi^{(2)}$ is the sum of the hyperpolarizabilities of all molecules. This can also be expressed in terms of the number density of the SHG-active molecules and their corresponding orientational average, $\langle\beta\rangle$. A detailed description of SHG theory in reflection mode and the algorithm which we used for analysis of our data can be found in Ref. [26]. The general equations [27] which relate the intensity of SHG light to the properties of the sample are simplified due to our experimental arrangement. In all our experiments the amphiphile adopts an azimuthal isotropic arrangement within the adsorption layer. As a result most of the 27 elements of the susceptibility tensor vanish and only two numerically independent elements remain. Furthermore we select molecules whose hyperpolarizability tensor of the SHG-active headgroup is dominated by its β_{zzz} component, which leads to further simplification.

For our experimental situation the following relation between the intensities $I^{2\omega}$ and I^{ω} can be derived. For an analyzer setting at $\hat{p}$ the following equation holds:

$$I^{2\omega} = D|(A\cos^2 P + C\sin^2 P)\chi^{(2)}_{zxx} + B\cos^2 P\chi^{(2)}_{zzz}|^2 I(\omega)^2 \ , \tag{8}$$

with

$$A = [F_z(2\omega)F_x(\omega) - 2F_x(2\omega)F_z(\omega)]F_x(\omega)\cos^2\alpha$$

$$B = F_z(2\omega)F_z^2(\omega)\sin^2\alpha$$

$$C = F_z(2\omega)F_y^2(\omega)$$

$$D = 4\left(\frac{\mu_0}{\epsilon_0}\right)^{3/2}\omega^2\tan^2\alpha \ ,$$

where P is the angle denoting the polarization of the fundamental with respect to the plane of incidence, α is the angle of incidence, μ_0 is the permeability constant and ϵ_0 is the permittivity constant. F_i refers to the Fresnel factor as derived by the boundary conditions at the interfaces and its value is determined by the dielectric function of the individual layer and α. The corresponding equation for an analyzer setting at $\hat{s}$ reads

$$I^{2\omega} = DF_y^2(2\omega)F_y^2(\omega)F_z^2(\omega)\sin^2(2P)|\chi^{(2)}_{yzy}|^2 I(2\omega)^2 \ . \tag{9}$$

Polarization-dependent measurements yield the unknown tensor elements and thus the corresponding molecular arrangement.

Experimental

Materials

The chemical formula of the soluble cationic amphiphile 1-alkyl-4-dimethylaminopyridinium bromide used in this study is presented in Fig. 1. The SHG activity is provided by the cationic headgroup with the dimethylamino group, $N(CH_3)_2$, acting as an electron donor. Details about the synthesis, analysis and various physical properties can be found in Ref. [28].

Sample preparation

An aqueous solution of the surfactant at a concentration close to the critical micelle concentration (cmc) was prepared using bidistilled water. This solution was then purified using a fully automated device described in Ref. [29]. The applied purification scheme ensures the complete removal of any surface-active impurities by repeated cycles of compression of the surface layer, its removal with the aid of a capillary, dilation to an increased surface area and the formation of a new adsorption layer. These cycles are repeated until the equilibrium surface tension, σ_e, between subsequent cycles remains constant. With this technique all trace impurities which might have an impact on the measurement are completely removed. Solutions at different concentrations were prepared by dilution of the stock solution.

Ellipsometry

All relevant design features of the ellipsometer (Multiskop, Optrel) are discussed in detail in Ref. [30]. We used the ellipsometry module in a nullellipsometer mode using a laser, polarizer, compensator, sample, analyzer arrangement. An average of zone I and III was used for the determination of the ellipsometric angles [14]. All measurements were carried out at an angle of incidence of 55° and a fixed wavelength of 632.8 nm. The resolution of the setting of the rotary stages was better than 1/200 of a degree; the extinction ratio of the polarizer was better than 10^{-8}. The corresponding imaging module was used for visualization of the morphology.

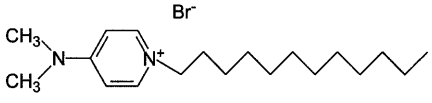

Fig. 1 Chemical structure of the cationic amphiphile used for the study

Second harmonic generation

SHG experiments were carried out in reflection mode at a fixed angle of incidence of 53°. The fundamental ($\lambda = 1064$ nm) of an active–passive mode-locked Nd-YAG laser (PY-61, Continuum), with a pulse width of 30 ps and a repetition rate of 12.5 Hz, was used as a light source and was focused with a lens on the sample. All spurious SHG created by the optical components was removed by a visible cutoff filter (RG630, Schott) placed just in front of the sample. The frequency-doubled light generated at the interface was separated from the fundamental using an IR cutoff filter (BG39, Schott) in conjunction with a narrow-band interference filter (532 BP, Instruments) and was subsequently detected by a photomultiplier (C83068, Burle) with a quantum efficiency of 15%. The signal was amplified (V5D, Seefelder Messtechnik) and processed by a 500 MHz, 2Gs/s digitizing oscilloscope (HP 54522A, Hewlett–Packard). A computer was used to control all vital elements of the experiment and also to perform the integration of the waveform. The SHG signal of a quartz crystal was used as a reference in order to eliminate experimental errors due to intensity fluctuations. The plane of polarization of the incident beam was rotated by a Glan laser polarizer (extinction ratio 10^{-6}, PGL, Halle) and a low-order quartz half-wave plate ($\Delta\lambda = 0.001$, RLQ, Halle) mounted on a motor-driven, computer-controlled rotary stage (M-445.21, Physik Instrumente). The polarization of the reflected SHG light was analyzed using a Glan–Thomson prism (extinction ratio 10^{-6}, Typ K, Steeg & Reuter).

Results and discussion

Special care was devoted to the preparation of the samples. Due to the peculiarities of surfactant synthesis, all surfactants contained trace impurities with a stronger surface activity than the main component. These trace impurities have no impact on any of the bulk properties; however, at the air–water interface they are enriched and may dominate the properties of the interfacial region. This was first recognized by Mysels [31] and there is experimental evidence that some peculiarities, for instance, an increase in the surface tension after micellation is caused by impurities. Our study requires the complete removal of all impurities. The equilibrium surface tension versus the bulk concentration of the purified system is shown in Fig. 2 and a detailed discussion can be found in Ref. [21].

The result of the purification is remarkable. Before purification the isotherm $\sigma \log c$ shows a pronounced linear dependence, while after purification the isotherm is shifted to lower values and exhibits a steadier increase in curvature. The very same changes were found for many other systems and hence some groups suggested that the quite frequently reported linear regime is simply an artefact caused by impurities [22]. However, despite the obvious impact of the purification on the isotherm, all purified systems can also be approximated just below the region of micellation by a straight line. The puzzle remains that a significant decrease in the surface tension of about 10 mN/m is observed in a range where the surface excess remains nearly constant. Further insight can be expected from dynamic experiments [23]. The relaxation of a nonequilibrium state should clarify if the subsurface layer contributes to the surface tension. Experiments which combine the technique of the oscillating bubble with SHG are currently in progress.

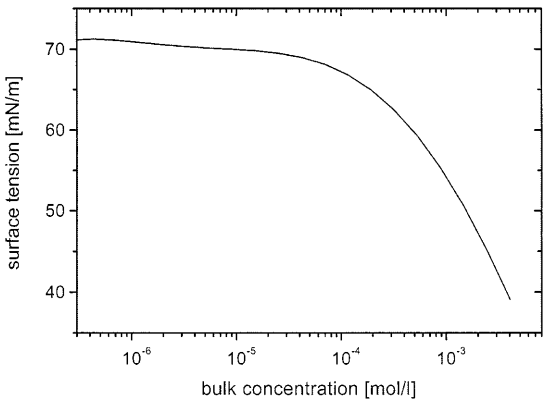

Fig. 2 The equilibrium surface tension, σ_e, of a purified aqueous solution of *N*-dodecyl-4-dimethylaminopyridinium bromide as a function of the bulk concentration, c

The adsorption layer was further characterized by imaging ellipsometry, which combines the high vertical sensitivity of ellipsometry with the lateral resolution of a light microscope. At all concentrations a homogeneous layer was found. Our model system behaves in all respects as other classical soluble amphiphiles do and also shows micellation. The system was then characterized by SHG. The most accurate determination of the susceptibility elements is obtained by polarization-dependent measurements. The plane of polarization of the linearly polarized fundamental beam is continuously rotated and the SHG response is measured at a fixed setting of the analyzer. A representative measurement of the SHG intensity $I^{2\omega}$ of an aqueous surfactant solution of concentration 4.16×10^{-3} mol/l is shown in Fig. 3. The squares represent the SHG data as measured and the solid lines refer to a fit, with the unknown elements of the susceptibility tensor being the fit parameter.

Figure 3a refers to an analyzer setting of $A = \hat{s}$. The absence of $\hat{s}$-polarized SHG light irrespective of incident $\hat{s}$ or $\hat{p}$ polarization of the fundamental is in agreement with an isotropic azimuthal distribution of the molecules. Figure 3b shows the corresponding data together with the model fit for an analyzer setting at $\hat{p}$ polarization. All measurements at different bulk concentrations possess the same features and the analysis reveals unambiguously that the orientation of the headgroup remains nearly constant for all bulk concentrations. This implies that the orientation of the headgroup is determined by the local environment and is, therefore, fairly independent of the packing of the aliphatic tails. The tilt angle, θ, was determined to be 49°, being defined in a way that $\theta = 0$ denotes an orientation parallel to the surface normal. A careful error analysis suggests an

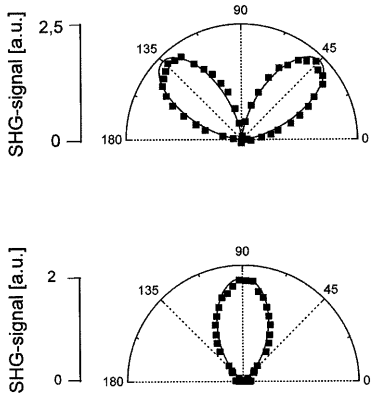

Fig. 3a, b Polar diagrams of the second-harmonic generation (*SHG*) intensity, $I^{2\omega}$, versus the plane of polarization of the linearly polarized fundamental beam. The *squares* represent the SHG data as measured and the *solid lines* refer to a model fit according to Eqs. (8) and (9) yielding the unknown elements of the susceptibility tensor. **a** was measured at a fixed analyzer setting of $A = \hat{s}$ and **b** shows the corresponding measurement for an analyzer setting of $A = \hat{p}$. The concentration of the solution was 4.16×10^{-3} mol/l

accuracy to within $\pm 2°$. A constant tilt angle over a wide range of surface concentrations appears to be peculiar but has also been reported for other soluble [32] as well as for some insoluble monolayers [33]. The experimental fact that there is no change in the orientational order simplifies the determination of the number density, N, of the surfactant within the adsorbed layer. SHG measurements with an analyzer setting at $A = \hat{s}$ depend only on the tensor element χ_{yzy} as can be seen from Eq. (9). χ_{yzy} is related to N and the orientational average of the hyperpolarizability of the adsorbed molecules by the oriented-gas model Eq. (7). Since the orientation remains constant at all bulk concentrations the intensity reading at a selected polarization setting is proportional to the number density: $\sqrt{I^{2\omega}(P = 45°,\ A = 90°)} \propto \chi_{yzy} \propto N$.

The absolute determination of N requires a proper calibration of the SHG intensity. A calibration is desirable since it is difficult to account for local field effects and can be achieved using Langmuir layers of a related insoluble compound with a longer alkyl tail. Both molecules possess the same headgroup which is responsible for the generation of SHG light. The electronic states of the headgroup are not altered by the length of the alkyl group and the local environment consisting of hydrated ions is comparable for both components as well. The selection of the right chain length turned out to be tricky. The C_{22} compound showed the formation of needles with compression and could not be used for calibration purposes; however, the π–A isotherm of the subsequently synthesized C_{20} compound possesses only a fluid expanded phase and imaging ellipsometry reveals a uniform and homogeneous film on a mesoscopic length scale. The corresponding isotherm is shown in Fig. 4 and the inset

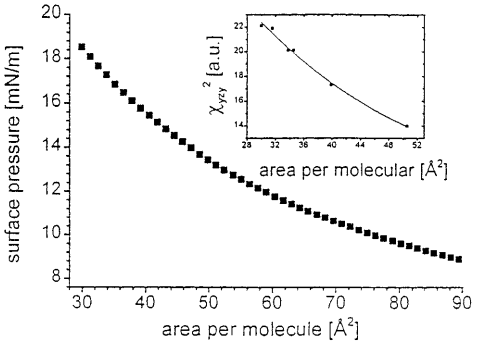

Fig. 4 π–A isotherm of N-eicosyl-4-dimethylaminopyridinium bromide (C_{20}). The *inset* shows the SHG intensity which was required for calibration purposes

represents the SHG intensity $\sqrt{I^{2\omega}(P = 45°,\ A = 90°)}$ in the particular range of interest. To make this calibration more sound and avoid misleading interpretations the calibration was repeated using a solution of the soluble surfactant as a subphase. A concentration just below the cmc was chosen and the signal recorded was identical within experimental accuracy. Consequently only the topmost monolayer contributes to the signal, which illustrates the high surface specifity of this technique.

The calibrated signal was then used to calculate the absolute number density of the soluble surfactant. The same quantity is determined by the analysis of the isotherm according to the Gibbs model and hence both approaches should lead to similar results. In Fig. 5 the slope of the isotherm is plotted versus the absolute number density as determined by the SHG measurements. Within experimental accuracy a linear relation is found. The factor m was used as a parameter in a least-squares fit and was found to be 1.28. Obviously this is closer to 1 rather than 2. This implies that the actual

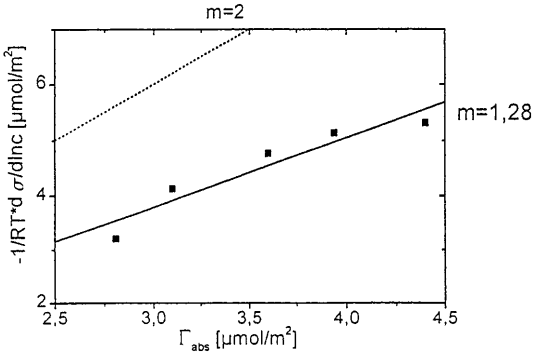

Fig. 5 The slope of the $\sigma(\ln c)$ isotherm is plotted versus the absolute surface excess as retrieved from the calibrated SHG signal. Both experiments determine the same quantity and can be used to determine the parameter m for a 1:1 electrolyte in the Gibbs equation. The factor m was determined to be 1.28. Also shown is a *straight line* which would hold if the factor were 2

m factor should not be taken for granted and thus depends on the nature of the ions involved.

The experimental findings can be explained by a modified Gibbs model. In the following we derive the Gibbs equation on the basis of a volume model. Our model takes into account the prevailing distributions of the ions within the surface phase, which leads to some modifications of the Gibbs equation. The interfacial phase possesses a thickness, h, and includes a Stern layer (inner and outer Helmholtz plane) with ions of a negative surfactant and counterions and an adjacent diffusion layer [34, 35]. The following notations are used in the analysis.

Γ_0^s: contribution of the Stern layer to the surface concentration of the solvent,
Γ_0: complete surface concentration of the solvent within the volume model,
Γ_-^v: surface concentration of the surfactant ions within the volume model,
Γ_s : contribution of the Stern layer to the surface concentration of the surfactant ions,
Γ_-: surface concentration of the surfactant ions according to the Gibbs equation,
Γ_+^v: surface concentration of the counterions within the volume model,
Γ_c : contribution of the Stern layer to the surface concentration of the counterions,
Γ_+: surface concentration of the counterions according to the Gibbs equation,
c_0 : volume concentration of the solvent,
c_b : volume concentration of the surfactant,
$c_-^s = c_-(h)$, $c_+^s = c_+(h)$: subsurface concentration of ions and counterions,
$n_0 = c_0/(c_0 + 2c_b)$: molnumber of the solvent,
$n = n_+ = n_- = c_b/(c_0 + 2c_b)$: molnumber of the surfactant ions and counterions.

The relations between the different surface concentrations are given by

$$\Gamma_0 = \Gamma_s + hc_0 \approx hc_0 \tag{10}$$

$$\Gamma_- = \Gamma_s + \int_0^h (c_-(x) - c_b)\mathrm{d}x \tag{11}$$

$$\Gamma_-^v = \Gamma_s + \int_0^h c_-(x)\mathrm{d}x \tag{12}$$

$$\Gamma_+ = \Gamma_c + \int_0^h (c_+ - c_b)\mathrm{d}x \tag{13}$$

$$\Gamma_+^v = \Gamma_c + \int_0^h c_-(x)\mathrm{d}x \ . \tag{14}$$

With these notations the Gibbs–Duhem equation of a completely dissociated bulk solution (T = constant)

$$n_0\mathrm{d}\mu_0 + n_-\mathrm{d}\mu_- + n_+\mathrm{d}\mu_+ = 0 \tag{15}$$

leads to

$$\frac{\partial\mu_0}{\partial c_b} = -\frac{n}{n_0}\left(\frac{\partial\mu_-}{\partial c_b} + \frac{\partial\mu_+}{\partial c_b}\right) \tag{16}$$

and, therefore, considering $c_0(n_-/n_0) = c_b$ and $c_0(n_+/n_0) = c_b$, the total differential of the surface tension (T = constant, electrical field vanishing for $x = h$) is of the form

$$\begin{aligned}
-\mathrm{d}\sigma &= \Gamma_0\mathrm{d}\mu_0 + \Gamma_-^v\mathrm{d}\mu_- + \Gamma_+^v\mathrm{d}\mu_+ \\
&= \left(-c_0 h\frac{n_-}{n_0} + \Gamma_s + \int_0^h c_-(x)\mathrm{d}x\right)\mathrm{d}\mu_- \\
&\quad + \left(-c_0 h\frac{n_+}{n_0} + \Gamma_c + \int_0^h c_+(x)\mathrm{d}x\right)\mathrm{d}\mu_+ \\
&= \left(\Gamma_s + \int_0^h (c_- - c_b)\mathrm{d}x\right)\mathrm{d}\mu_- \\
&\quad + \left(\Gamma_c + \int_0^h (c_+ - c_b)\mathrm{d}x\right)\mathrm{d}\mu_+ \ .
\end{aligned} \tag{17}$$

The (electro)chemical potential is independent of the thickness of the surface layer. Only the surface concentration, $\Gamma_\pm^v$, and the chemical standard potential of the surface layer are changed. The thickness of the interfacial layer should include the diffuse layer. With the electroneutrality condition and $\mathrm{d}\mu_- = \mathrm{d}\mu_+ = \mathrm{d}\ln c_b$, Eq. (17) leads to the Gibbs adsorption equation for ionic solutions:

$$\Gamma_- = -\frac{1}{2RT}\frac{\mathrm{d}\sigma}{\mathrm{d}\ln c_b} \tag{18}$$

which is invariant in the chosen thickness. The factor $m = 2$ in the Gibbs equation can be attributed to an increase in the osmotic pressure in the bulk phase as a result of the increase in number density due to the dissociation of the ions. These assumptions hold at low bulk concentration for our model system. Within a SHG measurement only Γ_s is measured; this exceeds Γ_- due to the potential in the diffusion sublayer. However, an estimation reveals that this is insufficient to account for the experimentally determined factor ($\Gamma_- - \Gamma_s \approx 1\%$ of Γ_-).

However, it is by no means obvious that all ions and counterions within the interfacial region can be considered as free particles. If some are coupled an additional term, $\Gamma_g\,\mathrm{d}\mu_g$, has to be introduced in Eq. (17) to describe the influence of these pairs on the surface tension. Equation (17) then reads

$$\begin{aligned}
-\mathrm{d}\sigma &= \Gamma_0\mathrm{d}\mu_0 + \Gamma_-^v\mathrm{d}\mu_- + \Gamma_+^v\mathrm{d}\mu_+ + \Gamma_g\mathrm{d}\mu_g \\
&= \left(2\Gamma_- + \Gamma_g\frac{\partial\mu_g}{\partial\mu_-}\right)\mathrm{d}\mu_- \ .
\end{aligned} \tag{19}$$

Here we have assumed that an equilibrium state exists between $\Gamma_- = \Gamma_+$ and $n_- = n_+$ and in addition between

Γ_-, Γ_+ and Γ_g. This means that $\mu_- = \mu_+$ and μ_0 have the same value in the bulk phase and in the interfacial phase, whereas Γ_g is only a function of the surface concentration $\Gamma_- = \Gamma_+$. Due to the prevailing molecular exchange between the bulk phase and the surface phase the derivative $\partial\mu_g/\partial\mu_-$ cannot easily be determined; however, the electrostatic repulsion in the Stern layer is reduced by coupling of ion and counterion. This in turn means that a greater number of headgroups are required to obtain the decrease in the surface tension (negative sign of $\partial\mu_g/\partial\mu_-$). As a consequence the factor in the Gibbs adsorption equation is reduced with trend to our experimental findings.

Our model system can also be used to determine the meaning of the ellipsometric quantity Δ and the result is shown in Fig. 6. As pointed out the square root of the SHG signal recorded at a polarizer setting of $P = 45°$ and an analyzer setting of $A = 90°$ is directly proportional to the number density of the amphiphile within the adsorption layer; it can therefore be used for an assessment of the meaning of Δ. If, as commonly assumed, the difference in Δ between the bare and the film-covered surface is directly proportional to the amount adsorbed a plot of $|\Delta - \Delta_0|$ versus χ_{yzy} should yield a straight line and the corresponding isotherms should possess similar features.

However, the analysis reveals major deviations between the two quantities. Figure 6 shows the ellipsometric signal $|\Delta - \Delta_0|$ versus the bulk concentration together with the SHG signal $\sqrt{I^{2\omega}(P = 45°,\ A = 90°)}$. The concentration of all the solutions is below the cmc and at least two independent runs were carried out for

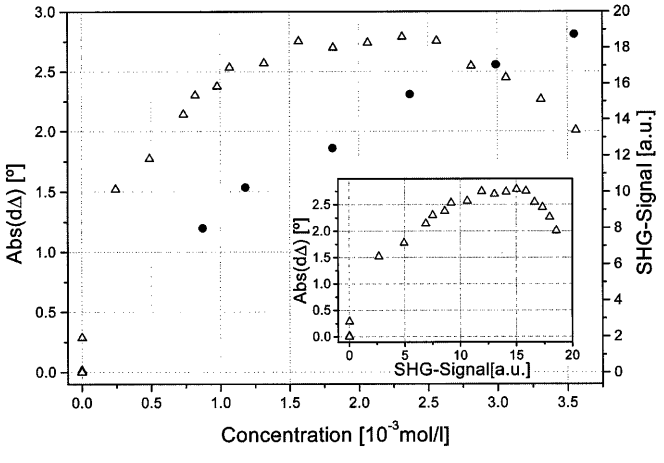

Fig. 6 Characterization of the equilibrium properties of the adsorption layer by ellipsometry and SHG. The SHG signal $\sqrt{I^{2\omega}(P = 45°,\ A = 90°)}$ (*circles*) is proportional to the surface excess and increases monotonously with the bulk concentration. The ellipsometric quantity $|\Delta - \Delta_0|$ (*triangles*) increases at low surface coverage with the concentration of the solution and shows a maximum at an intermediate concentration far below the critical micelle concentration

all measurements. The SHG response is proportional to the amount adsorbed and increases monotonously with the bulk concentration in accordance with the Gibbs model. The ellipsometric quantity $|\Delta - \Delta_0|$ increases at low surface coverage with the bulk concentration. At an intermediate bulk concentration $|\Delta - \Delta_0|(c)$ shows a maximum. A decrease in $|\Delta - \Delta_0|$ is observed even though there is a continuous increase in the surface excess, Γ. This clearly reveals that the ellipsometric quantity is not necessarily proportional to the amount adsorbed. Significant deviations may occur as shown for adsorption layers of soluble surfactants at the air–water interface. The model system is a typical representative of soluble amphiphiles and, therefore, we anticipate that these findings will hold on a more general basis.

There are two remarkable features of the ellipsometric measurements. First, there are already significant changes in Δ at very low bulk concentrations. Even submonolayer coverage causes pronounced changes in the optical properties. The surface excess at a bulk concentration of 2.5×10^{-4} is approximately 0.1 Γ_∞, as determined by SHG. Nevertheless $\Delta - \Delta_0$ amounts for three-fifths of $\Delta_\infty - \Delta_{max}$. The relation between Γ and $\Delta - \Delta_0$ is nonlinear and is very sensitive to the presence of amphiphiles. One of the best models for an optical description of submonolayer coverage is given by the effective-medium approximation [36]. This model yields the refractive index, which is, in our case, basically given by the volume fraction of the amphiphile within the adsorption layer. The observed changes in Δ are much bigger than predicted by this model. The water molecules in the interfacial area are differently bonded and oriented compared to those in the bulk phase. The transition layer accounts for a nonvanishing Δ value for the neat air–water interface. The presence of amphiphiles modifies the structure of the transition layer and leads to a specific ion distribution within the interfacial area; this influences the ellipsometric angle, Δ. A further quantification of this effect by adding an indifferent electrolyte was not possible since the electrolyte also changes the prevailing surface coverage and the structure of the monolayer.

The second surprising peculiarity of the system is a maximum in $|\Delta - \Delta_0|$ at an intermediate concentration far below the cmc. First, $|\Delta - \Delta_0|$ increases with bulk concentration and then decreases at an intermediate concentration. This observation can be understood semiquantitatively in terms of anisotropy effects. The molecules within the adsorption layer possess orientational order and polarization-dependent SHG measurements reveal a $C_{\infty v}$ arrangement of the amphiphiles' heads (and therefore most probably of the tails as well) within the adsorption layer. A proper optical model is provided by a uniaxial layer on an isotropic fluid. The complex reflectivity coefficient can again be expanded in a power series in terms of h/λ and the following

analytical expression for the change in Δ can be retrieved [37].

$$\Delta - \Delta_0 = -\left(\frac{4\pi h}{\lambda}\right) \frac{\sin\phi_0 \tan\phi_0 n_0}{1 - (n_0/n_2)^2 \tan^2\phi_0} \times \left[\frac{n_\perp^2 - n_2^2}{n_0^2 - n_2^2} - \frac{n_0^2}{n_\parallel^2}\left(\frac{n_\parallel^2 - n_2^2}{n_0^2 - n_2^2}\right)\right] . \quad (20)$$

The linear optical properties of the adsorption layer are mainly determined by the aliphatic tail of the amphiphile. The ratio of $n_\perp/n_\parallel$ depends on the orientation of the aliphatic tails. Simulations, using a set of reasonable optical constants, reveal that a change in the tilt of an aliphatic tail may account for the observed trend in $|\Delta - \Delta_0 CC|$. However, the observed changes are far bigger than effects which might be based on anisotropy effects. Further complications in the optical description of adsorption layers arise from the prevailing anisotropy within the surface layer. Slight changes in the orientational order lead to significant changes in Δ. A more quantitative analysis requires a reduction of the number of unknown parameters by independent means.

Summary and conclusion

The potential of ellipsometry and SHG for the characterization of adsorption layers of a soluble surfactant was discussed. SHG provides an intrinsic surface specificity and monitors only the state of the topmost monolayer. Data derived from SHG measurements were used for an assessment of thermodynamic models and our experiment required some modification of the underlying assumptions made in the Gibbs model. Limitations of optical techniques were also discussed. It was demonstrated that ellipsometry cannot be used for a precise determination of the surface excess. Nevertheless, it is still valuable to monitor qualitatively local and temporal variations of the molecular density at fluid interfaces. Our further research will be directed towards the dynamic aspect of monolayers and a combination of SHG with the technique of an oscillating bubble should provide insight into molecular transport mechanisms and help to understand aspects such as foam stability.

Acknowledgement The authors thank H. Möhwald for stimulating discussions.

References

1. Adamson AW (1993) Physical chemistry of surfaces. Wiley, New York
2. Möhwald H (1993) Rep Prog Phys 56:653
3. Miller R, Joos P, Fainermann V (1994) Adv Colloid Interface Sci 49:249
4. Gaines GL (1996) Insoluble monolayers at liquid–gas interfaces. Wiley, New York
5. Lunkenheimer K, Hirte R (1992) J Phys Chem 96:8683
6. Harke M, Goebel A, Prescher D, Lunkenheimer K, Motschmann H (1997) Langmuir 23:6274
7. Stauff J (1960) Kolloidchemie. Springer, Berlin Heidelberg New York
8. Gallardo BS, Mecalfe KJ, Abott NL (1996) Langmuir 12:4116
9. Joos P, Fang JP, Serrien G (1992) J Colloid Interface Sci 151:144
10. Kahlweit M, Busse G, Jen J (1991) J Phys Chem 95:5580
11. Lehmann S, Busse G, Kahlweit M, Stolle R, Simon F, Marowsky G (1995) Langmuir 11:1174
12. Bain CD (1998) Curr Opin Colloid Interface Sci 3:287
13. Möbius D (1996) Curr Opin Colloid Interface Sci 1:250
14. Azzam RM, Bashara NM (1979) Ellipsometry and polarized light. North Holland, Amsterdam
15. Lekner J (1987) Theory of reflection. Nijhoff, Boston
16. Reiter R, Motschmann H, Orendi H, Nemetz A, Knoll W (1992) Langmuir 8:1784
17. Motschmann H, Stamm M, Toprakcioglu C (1991) Macromolecules 24:3681
18. Teppner R, Bae S, Haage K, Motschmann H, Langmuir (1999) 15:7002
19. Shen YR (1989) Annu Rev Phys Chem 40:327
20. Corn RM, Higgins DA (1994) Chem Rev 94:107
21. Bae S, Haage K, Wantke D, Motschmann H (1999) J Phys Chem B 103:1045
22. Priester T, Bartoszek M, Lunkenheimer K (1998) J Colloid Interface Sci 208:5
23. Wantke K, Fruhner H, Fang J, Lunkenheimer K (1998) J Colloid Interface Sci 208:34
24. Vogel V, Mullin C, Shen YR, Kim MW (1995) J Chem Phys 95:4620
25. Prasad P, Williams DJ (1991) Introduction to nonlinear optical effects in molecules and polymers. Wiley, New York
26. Harke M, Ibn Elhaj M, Möhwald H, Motschmann H (1998) Phys Rev E 57:1806
27. Hirose C, Akamatsu N, Domen K (1992) Appl Spectrosc 6:1051
28. Haage K et al J Colloid Interface Sci (submitted)
29. Lunkenheimer K, Pergande HJ, Krüger H (1987) Rev Sci Instrum 58:2313
30. Harke M, Teppner R, Schulz O, Orendi H, Motschmann H (1997) Rev Sci Instrum 68:3130
31. Elworthy PH, Mysels KJ (1966) J Colloid Interface Sci 36:331
32. Hicks JM, Kemnitz K, Eisenthal KB, Heinz TF (1986) J Phys Chem 90:560
33. Berkovic G, Rasing T, Shen YR (1987) J Opt Soc Am B 4:945
34. Stern O (1924) Z Elektrochem 30:508
35. Kalinin VV, Radke CJ (1996) Colloids Surf A 114:337
36. Bruggeman D (1935) Ann Phys 24:637
37. Dignam M, Moskovits M, Stobie R (1971) Trans Faraday Soc 67:3306